

The width-amplitude relation of three-dimensional Bernstein-Greene-Kruskal electron solitary waves

Li-Jen Chen,¹ David J. Thouless,² and Jian-Ming Tang¹

¹*Department of Physics and Astronomy, University of Iowa, Iowa City, IA 52242-1479*

²*Department of Physics, University of Washington, Seattle, WA 98195-1560*

(Dated: December 17, 2018)

Three-dimensional Bernstein-Greene-Kruskal (BGK) electron solitary wave solutions are constructed for magnetized plasmas in which electrons are exactly magnetic field-aligned. The form of the solitary potential is not tightly constrained. If one takes a Gaussian form, the relation between the solitary potential amplitude and its parallel and perpendicular widths is constrained by an inequality. The inequality width-amplitude relation allows us to distinguish, based on macroscopic observables, the BGK solitary waves from other solitons such as Korteweg-de Vries solitons whose widths and amplitudes are of a one-one mapping relation. The inequality relation allows BGK solitary waves to be excited easily, since for a fixed amplitude there exists a wide range of admitted widths. When finite cyclotron radius effect is taken into account, the properties obtained for the case of zero cyclotron radius are found to be still applicable under the condition that the electron cyclotron radius is much less than the distance over which the structure of the solitary wave varies.

Long-lived coherent structures with nonuniform charge densities are ubiquitous in collisionless plasma systems. Laboratory experiments have shown that systems can be driven into states with such structures by applying voltages [1, 2], currents [3], waves [4], or beam injections [5]. In one dimension, general solutions of the time-stationary nonlinear Vlasov-Poisson equations that govern the electrostatic degree of freedom in collisionless plasma were first obtained by Bernstein, Greene, and Kruskal (BGK) [6]. These equations are nonlinear because the electrostatic potential is a function of particle distributions and that in turn determines how plasma particles distribute themselves. Nonuniform charge densities are sustained by this nonlinearity through the effect of particle trapping in the electrostatic potentials. In the linear regime where the deviation δf from the equilibrium distribution f_0 is small, $\delta f/f_0 \ll 1$ (or more precisely, $|\partial\delta f/\partial v| \ll |\partial f_0/\partial v|$), perturbed states with nonuniform charge densities would undergo Landau damping, and eventually relax to uniform states [7]. The BGK states, on the other hand, are nonlinear structures that are free from Landau damping.

We are interested in BGK waves that are fully localized in three dimensional space for magnetized plasma systems, and in the unique kinetic properties of these localized waves. Laboratory [1] and computer [8] experiments have shown that three dimensional BGK solitary waves are dynamically accessible from unstable initial conditions. Recent observations in collisionless space plasmas have also revealed the frequent appearance of electrostatic solitary structures that are fully localized [9, 10]. In this letter, we will first construct azimuthally symmetric solutions for the case of infinite magnetic field, derive the inequality width-amplitude relation, and discuss the uniqueness of having widths and amplitudes constrained by an inequality. We will then tune down the magnetic field to finite values and find conditions under which the

BGK solitary structures can be described by the solutions we constructed. We deal only with electron solitary waves in this paper, but similar calculations can be analogously applied to ion solitary waves.

To construct exact nonlinear solutions that are localized in three spatial dimensions, we use the BGK approach that was formulated for 1D nonlinear Vlasov-Poisson equations [6], and extend the Poisson equation to 3D. The electron solitary waves take the form of a potential hump. Electrons with total energy less than zero are trapped inside the potential energy trough, and are called trapped electrons. Electrons with positive energies are called passing electrons. Ions will be taken as uniform background, an approximation valid when the thermal energy of ions is much greater than that of electrons, or when the solitary waves move with respect to ions in a speed much larger than the ion thermal speed. We will prescribe the potential form and the passing electron distribution, solve for the trapped electron distribution, and derive the physical parameter range. It is much easier to do this than to prescribe the passing and trapped electron distributions to solve for the potential [11], so we can explore the allowed solitary wave solutions much more fully.

Using cylindrical coordinates (r, θ, z) with the symmetry axis \hat{z} defined to be along the direction of the background magnetic field, the dimensionless 3D Poisson equation with azimuthal symmetry takes the form

$$\left[\frac{\partial^2}{\partial r^2} + \frac{\partial}{r \partial r} + \frac{\partial^2}{\partial z^2} \right] \Phi(r, z) = -\rho(r, z), \quad (1)$$

where Φ is the dimensionless electrostatic potential normalized by T_e/e , where T_e is the parallel ambient electron thermal energy, ρ the dimensionless charge density, and lengths are normalized by the ambient parallel Debye length λ_D . With electrons moving only along \mathbf{B} , the dimensionless Vlasov equation for electrons written in the

wave frame becomes

$$v \frac{\partial f(r, z, v)}{\partial z} + \frac{1}{2} \frac{\partial \Phi(r, z)}{\partial z} \frac{\partial f(r, z, v)}{\partial v} = 0, \quad (2)$$

where v is the velocity along \hat{z} and is normalized by $v_{te} = \sqrt{2T_e/m_e}$. Because of azimuthal symmetry, there is no θ dependence in Φ and f . If the solitary wave moves with respect to the ambient electron frame, the ratio of the solitary wave speed to the thermal speed (called the Mach number) cannot be transformed away even in the wave frame, and will come in through the passing electron distribution. This point will be further illustrated when we get to the passing electron distribution.

Eq. (2) stipulates that for any r , there exists a 1D Vlasov equation in the parallel direction. These parallel Vlasov equations for different r are not independent, instead, their mutual relation in the perpendicular direction is determined by the perpendicular profile of Φ , due to the fact that Φ is the potential produced collectively by the plasma particles. Once Φ is known, the Poisson equation determines the electron density $\rho(r, z)$, the passing electron distribution $f_p(w)$ is determined by the Boltzmann distribution, and a trapped electron distribution $f_{tr}(w)$ can be found to make up the total density, where $w = v^2 - \Phi(r, z)$ is the electron energy. The important requirement for self-consistency is that the trapped electron distribution $f_{tr}(w)$ so determined should be non-negative. This procedure gives

$$\rho(r, z) = 1 - \int_{-\Phi}^0 dw \frac{f_{tr}(w)}{2\sqrt{w + \Phi}} - \int_0^\infty dw \frac{f_p(w)}{2\sqrt{w + \Phi}}. \quad (3)$$

If the potential $\Phi(r, z)$ (and thus ρ) and passing electron distribution $f_p(w)$ are known, the trapped electron distribution f_{tr} can be solved by inverting the integral. The important constraint that $f_{tr} \geq 0$ leads to the inequality width-amplitude relation. Neither the potential forms nor the passing electron distributions are tightly constrained. One can prescribe different localized potential functions [12] or different passing electron distributions (as long as the distribution functions satisfy the Vlasov equation) and obtain similar results on inequality width-amplitude relations. As an illustrating example, the solitary potential is chosen to be a double Gaussian,

$$\Phi(r, z) = \psi \exp\left(\frac{-z^2}{2\delta_z^2}\right) \times \exp\left(\frac{-r^2}{2\delta_r^2}\right), \quad (4)$$

where ψ is the potential amplitude, δ_z and δ_r are the parallel and perpendicular widths. The passing electron distribution is chosen to be Boltzmann distributed,

$$f_p(w) = \frac{2}{\sqrt{\pi}} \exp\left[-(\sqrt{w} \pm M)^2\right], \quad (5)$$

where $w = v^2 - \Phi(r, z)$ is the dimensionless total energy of an electron normalized by the ambient electron thermal energy, and M is the Mach number. In this letter,

we restrict to cases when solitary waves do not move in the ambient electron frame (zero Mach number). The finite Mach number cases will be treated elsewhere, but the main feature, namely that the width-amplitude relation is an inequality, we aim to address in this letter is independent of the Mach number.

With the potential and passing electron distribution given by Eqs. (4) and (5), the trapped electron distribution can be obtained from Eq. (3) as

$$\begin{aligned} f_{tr}(w; r, \psi, \delta_r, \delta_z) = & \frac{4r^2\sqrt{-w}}{\pi\delta_r^2} \left(\frac{1}{\delta_r^2} - \frac{1}{\delta_z^2} \right) - \frac{4\sqrt{-w}}{\pi} \left(\frac{2}{\delta_r^2} \right) \\ & + \frac{4\sqrt{-w}}{\pi\delta_z^2} \left[1 - 2 \ln \left(\frac{-4w}{\psi} \right) \right] \\ & + \frac{2 \exp(-w)}{\sqrt{\pi}} \left[1 - \text{erf}(\sqrt{-w}) \right], \end{aligned} \quad (6)$$

where $w = v^2 - \phi(r, z) < 0$. Different perpendicular, parallel widths and potential amplitudes give different constants and coefficients to $f_{tr}(w)$ and thus yield different f_{tr} values. Some combinations of $(\psi, \delta_r, \delta_z)$ can give negative f_{tr} values and this means that there does not exist an electron distribution to support the potentials with these $(\psi, \delta_r, \delta_z)$ parameters. To further illustrate how the tuning of the parameters affects the trapped electron distribution, the trapped and passing electron distributions f_{tr} (thick lines) and f_p (thin lines) are plotted at $r = 0$ and $z = 0$ as a function of velocity v in Figure 1. The parameters $(\psi, \delta_r, \delta_z) = (1.45, 5, 3)$ correspond to a BGK solitary wave that has zero phase space density at its phase space center ($r = 0, z = 0, v = 0$) as shown by the solid curves in Figures 1 (a) and (b). When the size of the structure is fixed, decreasing the amplitude raises the center phase space density as shown by the dashed curve for $\psi = 0.5$ in 1(a). On the other hand, increasing the amplitude would lower the center phase space density from zero to a negative value (not shown), and hence would result in unphysical solutions. When the amplitude is fixed, increasing the parallel size raises the center phase space density as shown in 1(b) by the dashed curve for $\delta_z = 10$. Varying δ_r results in a similar effect. The above examples also illustrate that when one prescribes a particular class of electron distributions with nonzero center phase space densities to solve for the potential, as Schamel did [11], one restricts to a small subset of the solution space. The width-amplitude relation obtained in [11] shows that the width decreases with increasing amplitude. This property was derived based on the solution subset, and is the property of that subset (depending on the location and shape of the subset in the entire solution space), not intrinsic to BGK solitary waves.

We now proceed to derive the width-amplitude inequality relation. For a given $w < 0$, the maximum r at which a trapped electron with energy $-w$ can exist is the r_{\max} that satisfies the condition $-w = \Phi(r_{\max}, 0)$.

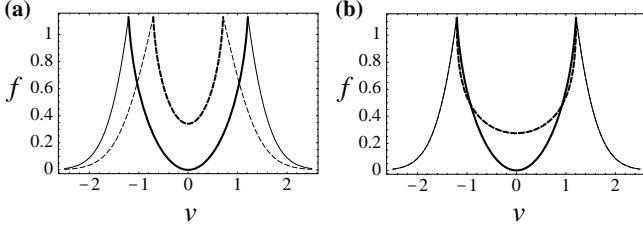


FIG. 1: Velocity distributions of electrons at the center ($r = 0, z = 0$) of BGK solitary structures for different potential amplitudes and sizes: (a) $(\psi, \delta_r, \delta_z) = (1.45, 5, 3)$ (solid lines) and $(\psi, \delta_r, \delta_z) = (0.5, 5, 3)$ (dashed lines), (b) $(\psi, \delta_r, \delta_z) = (1.45, 5, 3)$ (solid lines) and $(\psi, \delta_r, \delta_z) = (1.45, 5, 10)$ (dashed lines). In both cases the thick lines represent trapped electron distributions (Eq. (6)) for the specified parameters, and the thin lines are passing electron distributions (Eq. (5)).

Putting the Gaussian form of Φ into the condition, we obtain

$$r_{\max}^2 = -2\delta_r^2 \ln \frac{-w}{\psi}. \quad (7)$$

Since the condition $f_{tr}(w; r_{\max}) \geq 0$ guarantees $f_{tr}(w; r \leq r_{\max}) \geq 0$, to obtain the physical parameter range, we replace r^2 in $f_{tr}(w; r)$ by r_{\max}^2 . Reorganizing the terms in f_{tr} , we have

$$f_{tr}(w; r_{\max}) = \frac{2e^{-w}}{\sqrt{\pi}} [1 - \text{erf}(\sqrt{-w})] + \frac{4\sqrt{-w}}{\pi \delta_z^2} (1 - 4 \ln 2) - \frac{4\sqrt{-w}}{\pi} \left(\frac{2}{\delta_r^2} \right) \left[1 + \ln \left(\frac{-w}{\psi} \right) \right]. \quad (8)$$

As the global minimum of $f_{tr}(w; r_{\max})$ is $f_{tr}(w = -\psi; r_{\max})$, the condition of f_{tr} being nonnegative is ensured by $f_{tr}(w = -\psi; r_{\max}) \geq 0$. That is,

$$\frac{2e^{-\psi}}{\sqrt{\pi}} [1 - \text{erf}(\sqrt{\psi})] + \frac{4\sqrt{\psi}}{\pi \delta_z^2} (1 - 4 \ln 2) - \frac{4\sqrt{\psi}}{\pi} \left(\frac{2}{\delta_r^2} \right) \geq 0. \quad (9)$$

A re-arrangement of the above inequality yields

$$\delta_z \geq \sqrt{\frac{2(4 \ln 2 - 1)}{\sqrt{\pi} e^{\psi} [1 - \text{erf}(\sqrt{\psi})] / \sqrt{\psi} - 4 / \delta_r^2}}. \quad (10)$$

Figure 2 plots this inequality. Points lying on or above the shaded surface are allowed, and those under the surface are forbidden. The allowed region is marked by \circ and the forbidden region by \times . Curves on the $\delta_z = 0$ plane are projections of the constant δ_z contours to help visualization of the trend of the shaded surface. The shaded surface curves up toward ∞ because of the condition that the denominator inside the square-root sign in inequality (10) has to be positive, and that yields another inequality relation between δ_r and ψ . Inequality (10) stems from the fact that the overall profile of

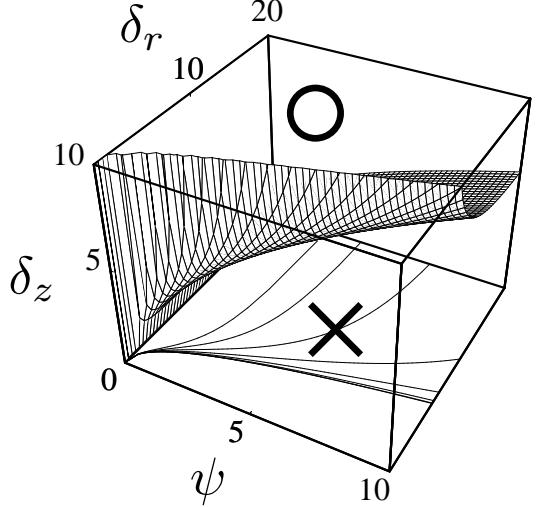


FIG. 2: The inequality relation between the parallel size (δ_z), the perpendicular size (δ_r) and the potential amplitude (ψ). The allowed region, the shaded surface and above, is marked by \circ and the forbidden by \times . The curves on the $\delta_z = 0$ plane are projections of constant δ_z contours on the surface.

$f_{tr}(w)$ is free to be shifted by an arbitrary positive number while maintaining it nonnegative. In other words, we have the freedom to adjust the occupation number of the trapped electron state, and this freedom manifests itself as the allowed continuum of widths and amplitudes on and above the shaded surface in Figure 2. A point on the shaded surface represents a parameter set that yields zero phase space density at $w = -\psi$, that is ($r = 0, z = 0, v = 0$), the center of the solitary phase space structure. One example of the empty-centered electron distribution has been provided in Figure 1 with the parameter set $(\psi, \delta_r, \delta_z) = (1.45, 5, 3)$. Lowering the amplitude or increasing the size shifts a point on the surface to the region above, and Figures 1(a) and (b) illustrate respectively the effects on the distribution functions.

In the limit of $\delta_r \rightarrow \infty$, the trapped electron distribution given by Eq. (8) reduces to the one-dimensional trapped electron distribution for a Gaussian potential and a Boltzmann passing electron distribution [13]. In this limit, the inequality width-amplitude relation is simply inequality (10) with δ_r set as ∞ . The 1D inequality relation provides us a ground to understand the discrepancy between the width-amplitude relations obtained by Turikov [14] and Schamel [11]. Turikov [14] studied only empty-centered electron holes and concluded that the potential width increases with the amplitude (correspond to points on the shaded surface in the limit $\delta_r \rightarrow \infty$), while Schamel [11] prescribed a class of trapped electron distributions whose center phase space densities always take positive values, and concluded that for small amplitude electron holes the width decreases with the amplitude. Schamel's conclusion was drawn from the obser-

vation that for smaller and smaller potential amplitudes, his β parameter picks up distributions with larger and larger center phase space densities, and therefore potential widths. These correspond to points in Figure 2 farther and farther above the shaded surface. The reader is referred to [15] for a more detailed discussion.

We now derive the condition under which the above properties can be carried over to the cases with finite magnetic field. We use the method based on studying the equations of motion of electrons in a uniform magnetic field by using the coordinates X, Y of the instantaneous center of the cyclotron orbit, and the components V_x, V_y of the velocity of the electron [16]. The motion of an electron inside the solitary structure, if we follow the electron, is influenced by the uniform \mathbf{B} and the 3D inhomogeneous $\mathbf{E}(x, y, z)$, where z is the coordinate parallel to \mathbf{B} . We want to know whether the effect of finite cyclotron radius would result in decoherence of the solitary structure, that is, how the distance of the guiding center to the symmetry axis would vary. Hence it is best to look at the electron motion on a 2D plane that is perpendicular to the magnetic field and onto which the 3D electron trajectory is projected. In the absence of the electric field, the solution of the equation of motion is

$$X = R \cos \alpha + \frac{V}{\omega} \cos(\phi + \omega t) \quad (11)$$

$$Y = R \sin \alpha + \frac{V}{\omega} \sin(\phi - \omega t), \quad (12)$$

where $\omega = eB/m$, R and α are polar coordinates of the gyro-center, V/ω the radius of the cyclotron orbit, ϕ the gyro-phase angle, and R, α, V, ϕ are constants. In the presence of the electric field (which shall be expressed as an electrostatic potential $U(\vec{r}, t)$, where the t -dependence is introduced by the z -dependence of $\mathbf{E}(x, y, z)$), the variables are no longer constants but vary with time. The equation for the most relevant variable R is

$$B\dot{R} = \frac{\partial U}{\partial r} \frac{V}{r\omega} \sin(\alpha - \phi - \omega t). \quad (13)$$

To the lowest order, integration of Eq. (13) gives the oscillatory solution

$$R = \left(\frac{\partial U}{\partial r} \right)_{r=R} \frac{V}{Br\omega^2} \cos(\alpha - \phi - \omega t) + R_0. \quad (14)$$

We therefore conclude that when the time variation scale of U is much smaller than the cyclotron frequency ω , and the spatial variation scale (r_U) of U is much smaller than the cyclotron radius r_c , the instantaneous guiding center would spiral around the zeroth order guiding center, and the solitary structure can be maintained. Since the time variation of U is characterized by the frequency of the electron bouncing in the parallel direction, the condition can be written as

$$\omega_b/\omega_c \ll 1 \rightarrow \sqrt{m_e \psi / e} \frac{1}{B\delta_z} \ll 1 \quad (15)$$

$$r_c/r_U \ll 1 \rightarrow \sqrt{2m_e \psi / e} \frac{1}{B\delta_r} \ll 1, \quad (16)$$

where we have expressed on the right hand side of the arrows the condition in terms of familiar variables. For a fixed potential amplitude ψ , the decrease in the magnetic field strength can be compensated by increases in δ_r and δ_z to keep the above two conditions satisfied. This would not be possible, had the width-amplitude relation been an equality. In other words, having the widths and amplitudes constrained by an inequality is essential for BGK solitary waves to exist with reasonable amplitudes in weak magnetic field regions such as the part of the magnetosphere that is farther away from the Earth. This result provides a basis to understand the fact that electrostatic solitary waves observed in the high latitude ionosphere where the magnetic field is weaker have larger size than those observed in the low latitude ionosphere [17].

The inequality width-amplitude relation distinguishes, based on macroscopic observables, BGK solitary waves from other solitons such as Korteweg-de Vries (KdV) solitons [18] whose width-amplitude relation is of one-one mapping. The size and the amplitude of BGK solitary waves do not have a lower cut-off within our theory. The size can be well below the Debye radius as far as there are enough electrons in the solitary wave to ensure the validity of the mean-field approach. Taking a Debye radius (λ_D) 100 m and a plasma density 5 cm^{-3} (typical of the low altitude auroral ionosphere), a width of 0.01 λ_D for the solitary potential allows 5×10^6 electrons in the structure, and hence is still well within the functioning range of the mean-field approach. Indeed, subDebye scale solitary waves have been observed [10].

In summary, we have constructed azimuthally symmetric BGK electron solitary wave solutions when electrons only travel along the magnetic field, derived the inequality width-amplitude relation, and obtained the condition under which the results for zero cyclotron radius are applicable to the cases with finite cyclotron radius. The facts that the potential forms are not tightly constrained and that the width-amplitude relation is an inequality provide a multitude of freedom for the BGK solitary structures to exist, and make BGK solitary waves easily accessible in systems with sufficiently high fluctuation levels. From this point of view, it is not surprising that BGK waves are ubiquitous in driven and turbulent plasma systems where collisional effect is negligible. A high probability of excitations of the BGK solitary waves is expected to alter the bulk properties of the plasma medium such as the dc resistivity.

The research at the University of Iowa is supported by the DOE Cooperative Agreement No. DE-FC02-01ER54651, and at the University of Washington by NSF DMR-0201948.

[1] J. P. Lynov *et al.*, Phys. Scr. **20**, 328 (1979)

[2] G. Bachet *et al.*, Phys. Plasmas **8**, 3535 (2001)

[3] C. Chan *et al.*, Phys. Rev. Lett. **52**, 1782 (1984)

[4] D. S. Montgomery *et al.*, Phys. Rev. Lett. **87**, 155001 (2001)

[5] H. Klostermann and Th. Pierre, Phys. Rev. E **61**, 7034 (2000)

[6] I. B. Bernstein, J. M. Greene, and M. D. Kruskal, Phys. Rev. **108**, 546 (1957)

[7] L. Landau, J. Phys. **10**, 25 (1946)

[8] N. Singh, *et al.*, Geophys. Res. Lett. **27**, 2469 (2000)

[9] J. R. Franz, P. M. Kintner, and J. S. Pickett, Geophys. Res. Lett. **25**, 1277 (1998)

[10] R. E. Ergun, *et al.*, Phys. Rev. Lett. **81**, 826 (1998)

[11] H. Schamel, Phys. Scr. **T2/1**, 228 (1982)

[12] L.-J. Chen and G. K. Parks, Geophys. Res. Lett. **29**(9), 10.1029/2001GL013385 (2002)

[13] L.-J. Chen and G. K. Parks, Nonlinear Processes in Geophys. **9**, 111 (2002)

[14] V. A. Turikov, Phys. Scr. **30**, 73 (1984)

[15] L.-J. Chen, PhD dissertation, University of Washington (2002)

[16] M. H. Johnson and B. A. Lippman, Phys. Rev. **76**, 828 (1949)

[17] C. A. Cattell *et al.*, Geophys. Res. Lett. **26**, 425 (1999)

[18] H. Washimi and T. Taniuti, Phys. Rev. Lett. **17**, 996 (1966)